



Geochemistry and Petrography of the Sediments From the Marginal Areas of Qinghai Lake, Northern Tibet Plateau, China: Implications for Weathering and Provenance

Huifei Tao^{1*}, Lewei Hao^{1*}, Shutong Li¹, Tao Wu², Zhen Qin^{1,3} and Junli Qiu¹

¹Oil and Gas Research Center, Northwest Institute of Eco-Environment and Resources, Chinese Academy of Sciences, Lanzhou, China, ²Research Institute of Exploration and Development, Petrochina Xinjiang Oilfield Company, Karamay, China, ³University of Chinese Academy of Sciences, Beijing, China

OPEN ACCESS

Edited by:

Yongli Wang,
Key Laboratory of Cenozoic Geology
and Environment, Institute of Geology
and Geophysics, (CAS), China

Reviewed by:

Duofu Chen,
Shanghai Ocean University, China
Yougui Song,
Institute of Earth Environment, (CAS),
China

*Correspondence:

Huifei Tao
tophic3@yeah.net
Lewei Hao
lwhao@lzb.ac.cn

Specialty section:

This article was submitted to
Quaternary Science, Geomorphology
and Paleoenvironment,
a section of the journal
Frontiers in Earth Science

Received: 15 June 2021

Accepted: 25 August 2021

Published: 15 September 2021

Citation:

Tao H, Hao L, Li S, Wu T, Qin Z and
Qiu J (2021) Geochemistry and
Petrography of the Sediments From
the Marginal Areas of Qinghai Lake,
Northern Tibet Plateau, China:
Implications for Weathering
and Provenance.
Front. Earth Sci. 9:725553.
doi: 10.3389/feart.2021.725553

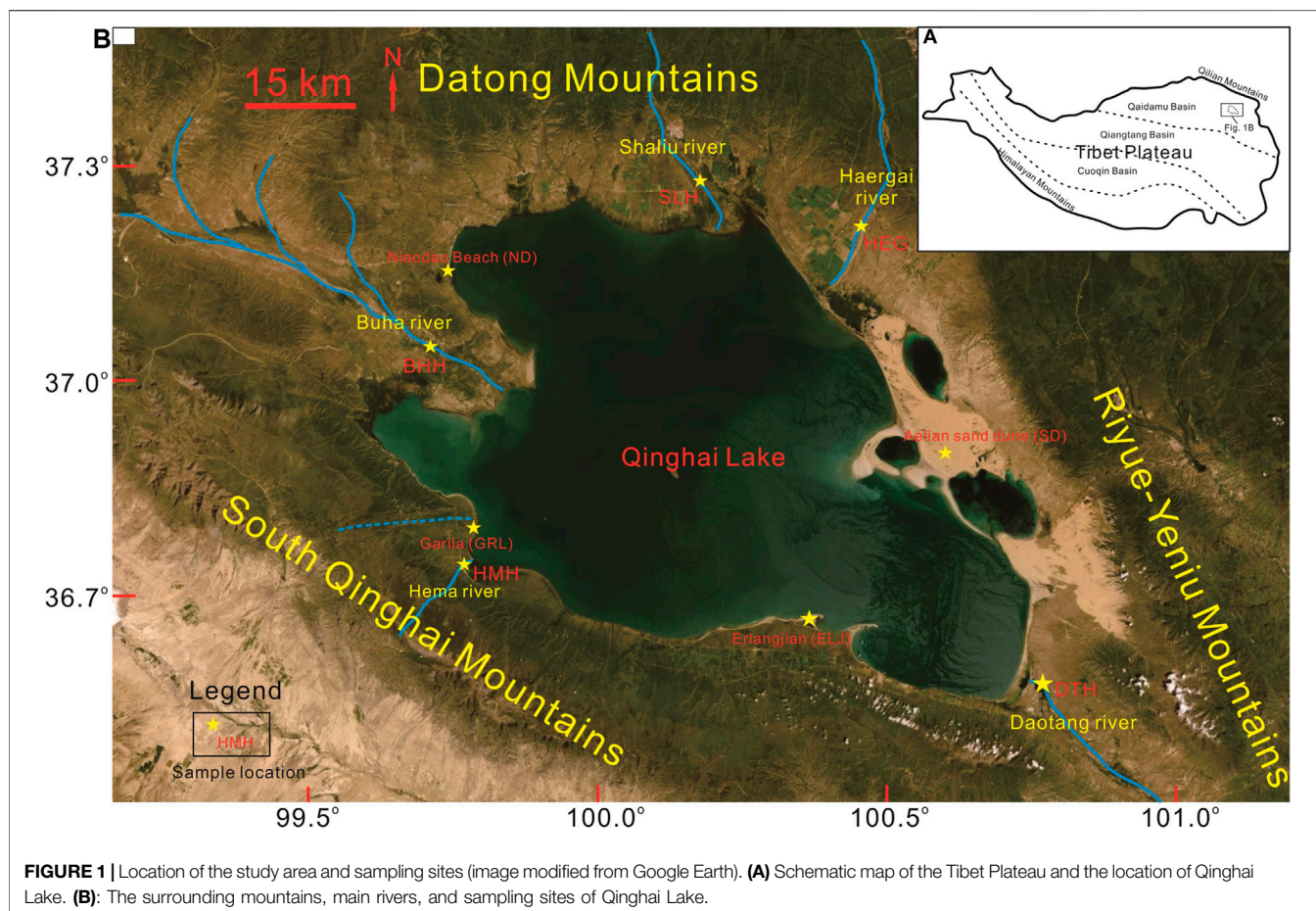
The provenance study of the sediments from Qinghai Lake is of great significance for the understanding of geological and climatic evolution processes of the Tibet Plateau on the one hand and for evaluating the controlling factors of the sediment components on the other hand. The samples were collected from five rivers, foreshore, beach, beach bar, and aeolian sand dune in the Qinghai Lake. The bulk geochemical composition, petrography, and mineralogy features of the samples are analyzed. The results show that: 1) Qinghai Lake sediments experienced low-intensity chemical weathering from the source areas to the deposition sites and were affected by some recycled detrital materials and 2) the source rocks for the sediments include felsic rocks (granite, granodiorite, and felsic volcanic rocks), carbonate, metamorphic rocks (marble and meta-volcanic rocks), and clastic rocks with the felsic source rocks to have the most important impact on the chemical compositions of the sediments. The geochemical indicator of Al_2O_3/TiO_2 reflects that the provenance of fine-grained sediments from the center of Qinghai Lake is more mafic than the coarse-grained sediments from the margin of the Qinghai Lake, suggesting that the hydraulic sorting of grain size probably plays an important role in the geochemical compositions of the sediments. The mafic elements were probably preferentially enriched in muds.

Keywords: Qinghai Lake, geochemical compositions, weathering, provenance, hydraulic sorting

INTRODUCTION

Qinghai Lake is the largest inland closed salinized lake, located at the Northern Tibet Plateau (Figure 1A). The formation of Qinghai Lake was closely associated with the uplift of the Tibet Plateau. The Qinghai Lake rift valley was declined and the mountains were rapidly uplift because of the Himalayan movement during the Late Neogene to Holocene (An et al., 2006; Chang et al., 2008).

The thicknesses of the sediments in the southern and northern depressions of Qinghai Lake are over 700 and 560 m (An et al., 2006). The uninterrupted sediments are sensitive to the changes of climate and tectonic, making Qinghai Lake a natural laboratory for the study of climate and tectonic evolution of the Tibet Plateau. There have been a few research projects carried out on Qinghai Lake,



for example, “Comprehensive survey of Qinghai Lake, 1979” (Lanzhou Institute of Geology CAS, et al., 1979) and “Qinghai Lake Environmental Drilling, 2003” (An, 2003). The basement structures, the geochemical and mineral compositions of the drilled core and bottom sediments, and water chemical ions of Qinghai Lake were investigated (Zhang et al., 1994; Liu et al., 2002; Jin et al., 2009, 2015; Xiao et al., 2012; Zhang et al., 2019; Song et al., 2020). And the hydroclimate changes were reconstructed in Qinghai Lake since the last glacial period (Jin et al., 2009, 2015; Song et al., 2020). However, the previous work paid more attention to the sediments from the center of the Lake, while the terrestrial detritus in the margin of Qinghai Lake (main streams, beach bars, and sand dunes) are less concerned. The sediments from the margin of Qinghai Lake primarily reflected the signals of the source areas because the sediments from the marginal areas are barely affected by the water environment of the lake without post-depositional diagenesis. Thus, the sediments from the margin of Qinghai Lake are ideal materials to trace the source rocks of Qinghai Lake and to evaluate the influence of the hydraulic sorting.

The concentrations of some elements (e.g., Al, Ti, Th, Sc, Cr, Co, La, Zr, and Hf) and their ratios and petrography of the sediments are widely used to trace the provenance of the siliciclastic rocks (Cullers, 2002; Hofmann et al., 2003; Wanas and Abdel-Maguid, 2006; Pe-Piper et al., 2008; Lee, 2009;

Armstrong-Altrin et al., 2012; Schneider et al., 2016; Qiu and Zou., 2020; Rahman et al., 2020). The geochemistry and mineralogy constituents of the sediments are controlled by the source rock types, weathering conditions, transportation, and post-depositional diagenesis processes (McLennan et al., 1993). The previous research suggested that the physical sorting of sediment during the processes of transport and deposition leads to the concentration of quartz and feldspar with some heavy minerals in the coarse fraction and the secondary lighter and more weatherable minerals in the suspended-load sediments, which causes the chemical index of alteration (CIA) increasing along with decreasing grain-size fractions (Armstrong-Altrin et al., 2004).

The surface sediments from Qinghai Lake are experiencing low-intensity chemical conditions because of the cold and dry climate in the Tibet Plateau (Liu et al., 2002; Chang et al., 2008; Jin et al., 2009) and diagenesis barely happened. Therefore, the geochemistry and mineral compositions of the sediments from Qinghai Lake reflect the features of the source rocks and also can be used to analyze the influence of the physical sorting. In this study, elements, minerals, and petrography features are analyzed for the sediment samples from five main rivers, beach, beach bar, and sand dune of the Qinghai Lake. Then, the weathering conditions and source rock types of the provenance were discussed, and the indicators for the provenance study were

also evaluated combined with previous studies and the geological setting.

GEOLOGICAL SETTING

Qinghai Lake is located at the northern Tibet Plateau (**Figure 1A**), the biggest inland lake in China, and it is an enclosed rift lake constrained by surrounding mountains, approximately diamond-shaped with a 106 km NWW direction long axis and a 63 km short axis. Its circumference is about 360 km and covers an area over 4,000 km² with an altitude of ca. 3,200 m. The maximum water depth of Qinghai Lake is 28.70 m with an average depth of 19.15 m (Lanzhou Institute of Geology CAS, et al., 1979). Qinghai Lake belongs to a typical high altitude, cold and arid continental climate, and less rainfall. The evaporation in Qinghai Lake is greater than the sum of rainfall and runoff into the lake; thus, the salinity of the water increases and the area of the lake becomes smaller gradually, and the water level and lake area gradually declined to their minima in 2004 (Dong et al., 2019). With the increasing of annual rainfall and temperature, the water body of Qinghai Lake has been expanded since 2004 (Dong et al., 2019).

Qinghai Lake was formed due to the Late Himalaya neotectonic movement (Yuan et al., 1990). Before the Middle Pleistocene, Qinghai Lake was narrow and shallow, as a transit lake of the Paleo-Buha River to Daotang River, and finally flowed east to the Yellow River. From the Middle to Late Pleistocene, the basin of Qinghai Lake continuously fell and the Riyue-Yeniu mountains uplift in the east, cutting off the connection between the Paleo-Buha River and the Yellow River. Thus, all the rivers flow into Qinghai Lake and make it a closed inland lake since the Late Pleistocene.

There are five relatively big and perennial flow rivers developed in Qinghai Lake (**Figure 1B**). Three of them (Buha River, Shaliu River, and Haergai River) are to the northwest of the lake with another one (Heima River) in the south of and the other (Daotang River) coming from the southeast. The Daotang River flows into the lagoon of Erhai located in the southeast of Qinghai Lake. The Buha River has the biggest runoff and maximum sediment inputs among all the rivers, occupying ca. 67% of the total sediment inputs into Qinghai Lake (Li et al., 2010). Deltas, abandoned channels, alluvial fans, and near-shore deposits (e.g., beach, beach bars, aeolian dunes, and barrier islands) develop around the Qinghai Lake.

The Datong Mountain was located to the west and northwest of Qinghai Lake while the Riyue-Yeniu mountains and Qinghai South Mountain are situated at the east and south of Qinghai Lake, respectively (**Figure 1B**). The drainage of the Buha River is mainly distributed in the southern Datong Mountain and consists of Silurian granodiorite and monzonite, Lower Silurian meta-sandstone and slate, and Middle to Late Triassic limestone and clastic rocks. The Shaliu River runs out of the western Datong Mountain and flows through the Permian and Triassic marine siliciclastic rocks and Silurian biotite granite. The Haergai River originates from the east of the Datong Mountain, where the Sinian slate, dolomite and clastic rocks, the Cambrian to Ordovician marble, meta-volcanic and schist, the Silurian biotite granite, and a few Permian and Jurassic clastic rocks

are cropped out. The water system of the Daotang River mainly originated from the Riyue-Yeniu mountains, which consist of Permian granites and Triassic clastic rocks and limestone. The Heima River comes from the South Qinghai Mountain, which is mainly composed of Carboniferous clastic rocks and limestone, Triassic felsic volcanic rocks and clastic rocks, and Late Triassic granodiorite including many gabbros and pyroxenite xenoliths (QBGMR, 1991; Chen, 2016).

MATERIALS AND METHODS

Five sand samples were collected from the five relatively big rivers (Buha River, Shaliu River, Haergai River, Heima River and Daotang River, marked by BHH, SLH, HEG, HMH, and DTH) and one sample was collected from the beach close to an unknown river mouth near the village of Garila to the south of the lake (marked by GRL). Eight sand samples were collected from the Erlangjian beach bar to the southeast of the lake (marked by ELJ1-8), eight sand samples were collected from the beach of Niaodao (marked by ND1-8), and six sand samples were collected from the aeolian sand dune to the northeast of the lake (marked by SD1-6) (**Figure 1B**).

Thirty-two thin sections were prepared for petrography study. The unconsolidated sands were immersed by using epoxy resin and a curing agent on the electric hot plate. When the epoxy resin was totally soaked into the samples, the samples were transferred to a 60–70 centigrade oven for 4–5 h to solidify the samples. After that, the solidified samples were cut into 0.03 mm thick sections. Fifteen samples from the Erlangjian (ELJ) beach bar and Niaodao (ND) beach were ground into 200 mesh (<0.075 mm) for X-ray diffraction (XRD) analysis which was performed on an Empyrean X-ray diffractometer using Cu Ka radiation at 40 kV and 40 mA. Each scan was performed from 5° to 45°, with a step interval of 0.02° at a rate of 2.0°/min.

Major elements were determined using X-ray Fluorescence Spectrometry (XRF) at Lanzhou University. The sample powders (<0.075 mm) were dried in an oven at 105°C. 4 g of the dry powdered samples are pressed into a 32 mm diameter pellet using 30-ton pressure using the pressed powder pellet technique. The briquettes were then stored in desiccators. Calibration curves were established using the reference materials of rock (GSR01-GSR12). Analytical uncertainties are ±5% for all major elements except for P₂O₅ and MnO (up to ±10%). 40 mg powdered samples were weighed for trace elements analysis by using inductively coupled plasma mass spectrometry (ICP-MS, Nu Attom). The processing and analytical procedures for trace elements were as described in Li (1997). The precision for most trace element measurements is estimated to be 5% according to the analysis of the GSR1 and GSR3 standards.

RESULTS

Petrology and Mineralogy

The results of thin-section observation show that the mineral compositions of the sands in the Qinghai Lake

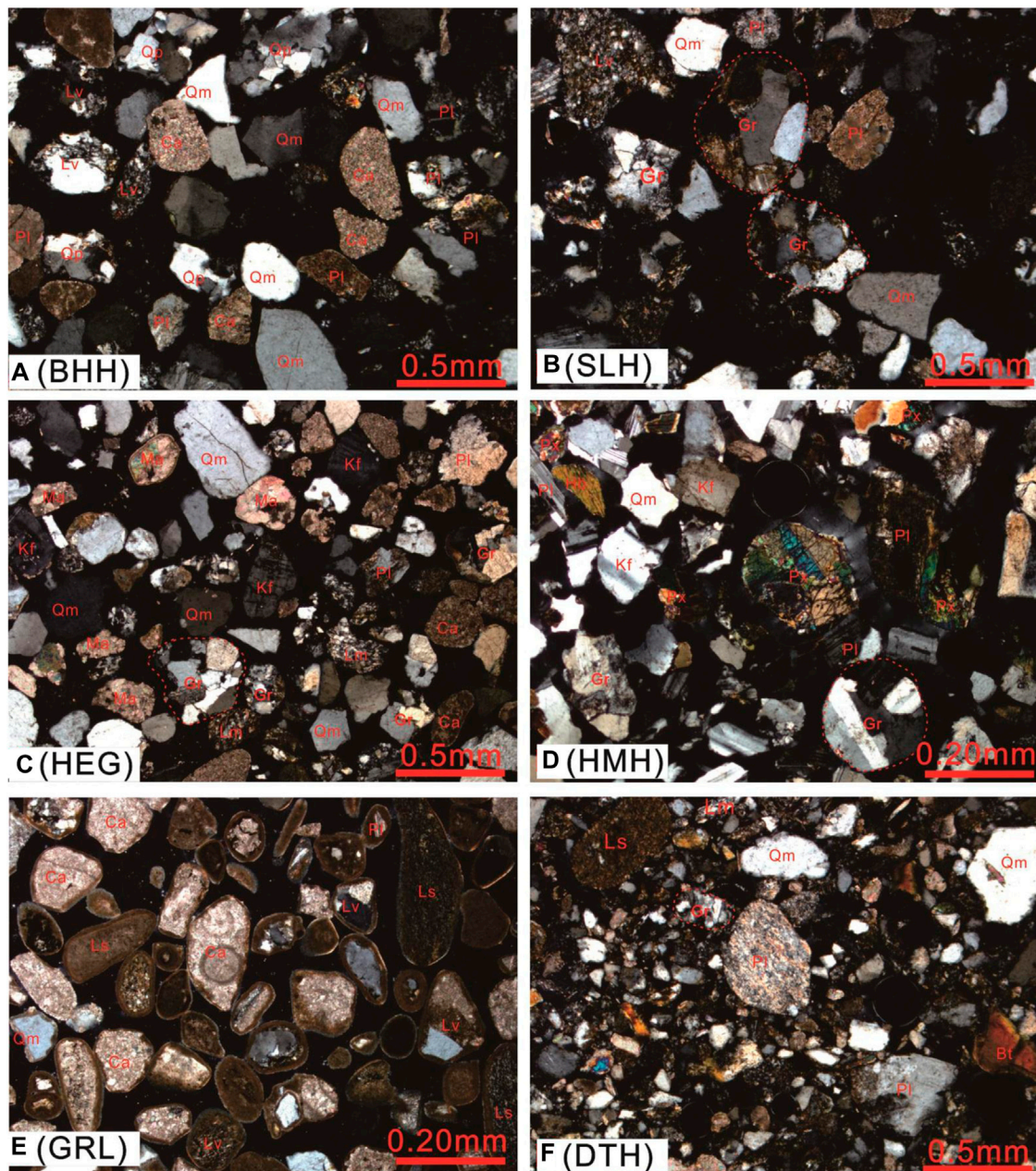


FIGURE 2 | Photomicrographs of the sand sediments from the rivers of Qinghai Lake, cross-polarized light. **(A)** Sands from Buha River (BHH). **(B)** Sands from Shaliu River (SLH). **(C)** Sands from Shaliu River (SLH). **(D)** Sands from Heima River (HMH). **(E)** Sands from foreshore near Garila village (GRL). **(F)** Sands from Daotang River (DTH). Qm: monocrystalline quartz, Qp: polycrystalline quartz, Lv: volcanic fragment, Lm: metamorphic fragment, Ls: sediment fragment, Gr: granite fragment, Ca: calcite minerals, Pl: plagioclase, Kf: K-feldspar, Ma: marble, Hb: hornblende, Px: pyroxene, Bt: biotite.

are mainly feldspar, quartz, lithic fragments, biotite, marble, pyroxene, and hornblende (**Figure 2** and **Figure 3**). The lithic fragments include carbonate, metamorphic rocks, granite, volcanic rocks, and fine clastic rocks. The monocrystalline quartz and feldspar minerals are ubiquitous in the sediments. However, the types and proportions of some minerals in the samples from different sites vary greatly. The sediments of BHH have

the highest polycrystalline quartz contents among all the sample sites (**Figure 2A**), whereas the SLH and HEG samples have abundant granite fragments and a few metamorphic rocks (**Figures 2B,C**). The sample HMH contains relatively high concentrations of pyroxene and hornblende minerals (**Figure 2D**), and the sample GRL shows remarkably high carbonate debris (**Figure 2E**), and some biotite minerals present in the sediments of the DTH

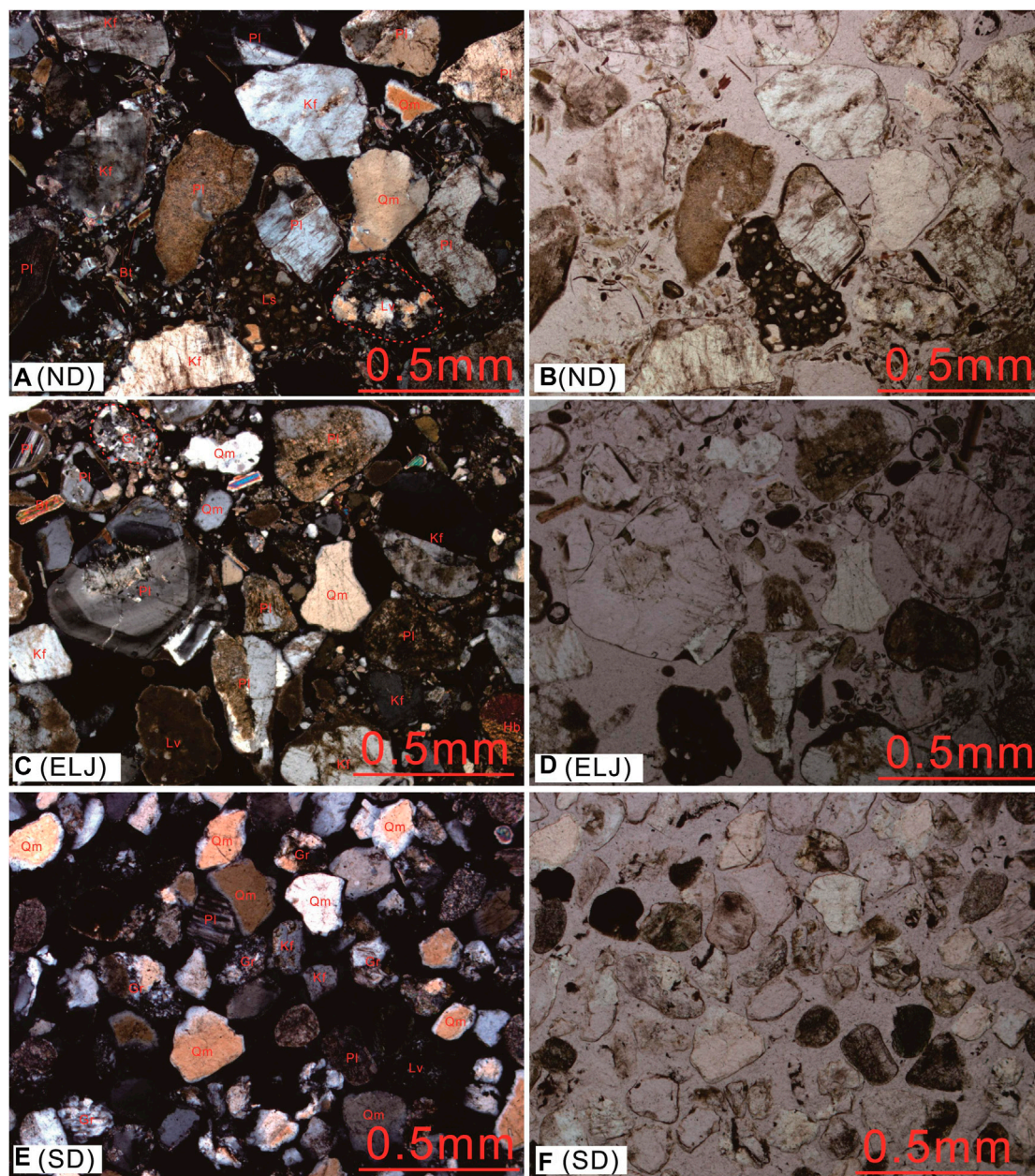


FIGURE 3 | Photomicrographs of the sand sediments from the beach, beach bar, and aeolian sand dune of the Qinghai Lake, cross-polarized light (**left**) and plane-polarized light (**right**). (**A, B**) Sands from the Niaodao beach (ND). (**C, D**) Sands from the Erlangjian beach bar (ELJ). (**E, F**) Sands from the aeolian sand dune (SD). Qm: monocrystalline quartz, Lv: volcanic fragment, Ls: sediment fragment, Gr: granite fragment, Pl: plagioclase, Kf: K-feldspar, Hb: hornblende, Bt: biotite.

(**Figure 2F**). The sediments from the rivers are well-sorted, except for the sample DTH, and the detrital grains from the rivers are angular to subangular roundness, whereas the sample from the beach (GRL) has relatively good sorting and roundness. Compared with the sediments in the rivers, the samples in the ELJ beach bar, ND beach, and sand dune (SD) have more feldspars and fewer lithic fragments (**Figure 3**). The mica minerals (including biotite and muscovite) are commonly seen in the ELJ beach bar and ND beach samples (**Figures 3A–D**).

The results of X-ray diffraction analysis of the samples from ELJ beach bar and ND beach are list in **Supplementary Appendix Table S1**. The primary mineral compositions are quartz (31–55%, avg. 43.75%), K-feldspar (5–31%, avg. 12.4%), plagioclase (11–32%, avg. 19.7%), clay (4–20%, avg. 8.4%), calcite (1–8%, avg. 3.8%), dolomite (1–4%, avg. 2.2%), pyroxene (2–8%, avg. 3.7%), and hornblende (1–14%, avg. 4.9%) with a few siderite and other minerals. The significant features are the abundant feldspar minerals that existed in the area of ELJ beach bar and ND beach with a total feldspar proportions' range from 19 to 48%, avg. 32% (**Figure 4**).

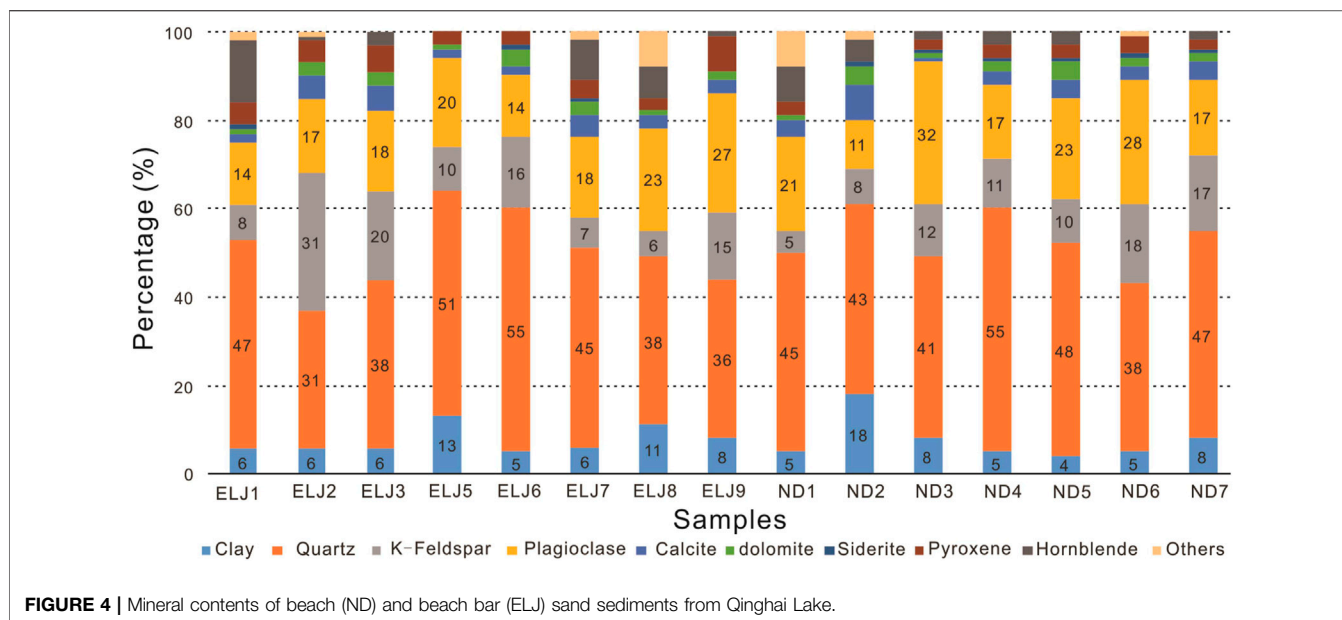


FIGURE 4 | Mineral contents of beach (ND) and beach bar (ELJ) sand sediments from Qinghai Lake.

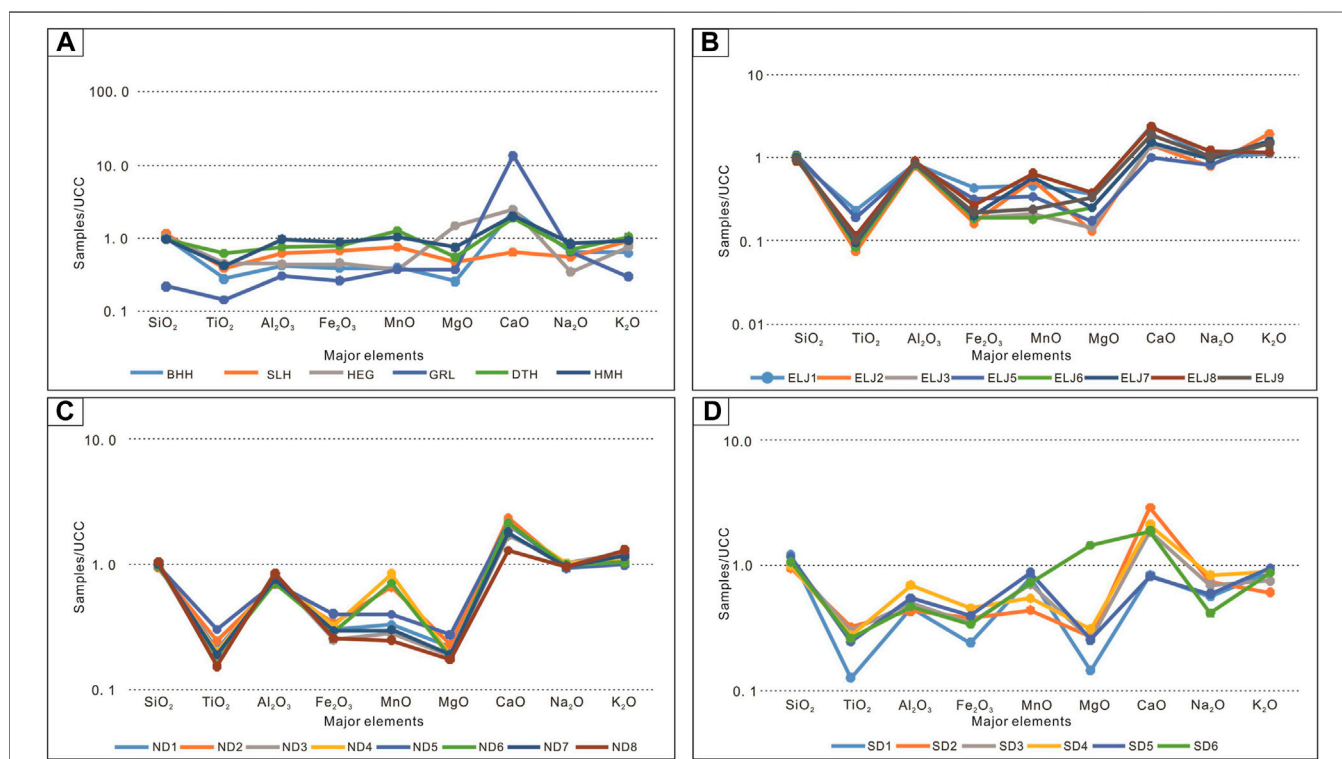


FIGURE 5 | UCC-normalized spider diagrams of major elements for different samples from the Qinghai Lake area. (A) Samples from rivers and GRL foreshore, (B) samples from Erlangjian beach bar (ELJ), (C) samples from Niadao beach (ND), and (D) samples from aeolian sand dune (SD), respectively.

Major Elements

Overall, the Upper Continental Crust (UCC) (Rudnick and Gao, 2003) normalized spider diagrams show that the major element contents of the samples from the rivers and GRL vary greatly, whereas the major elements of the samples from the ELJ beach

bar, ND beach, and SD are more uniform (Figure 5). Compared with UCC, most of the samples from the rivers and GRL have comparable or lower SiO₂, TiO₂, Al₂O₃, Fe₂O₃, MnO, and MgO and higher CaO, except for sample SLH (Figure 5A). Sample SLH shows a lack of CaO, which is consistent with the barely observed

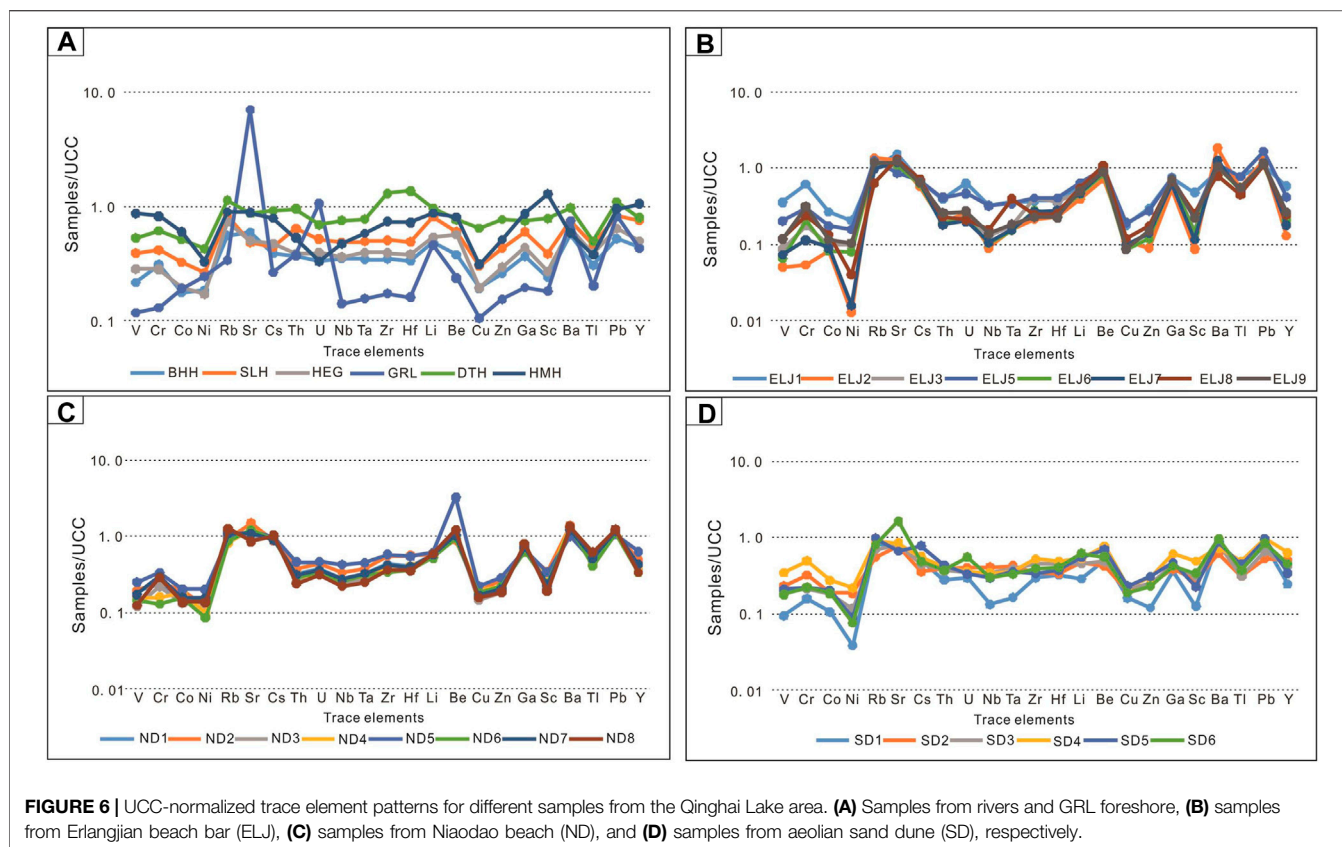


FIGURE 6 | UCC-normalized trace element patterns for different samples from the Qinghai Lake area. **(A)** Samples from rivers and GRL foreshore, **(B)** samples from Erlangjian beach bar (ELJ), **(C)** samples from Niaodao beach (ND), and **(D)** samples from aeolian sand dune (SD), respectively.

amount of carbonate debris in the thin section (**Figure 2B**). The samples from ELJ beach bar and ND beach show similar SiO_2 and Na_2O with UCC, but slightly enriched in CaO and K_2O and depletion of TiO_2 , Al_2O_3 , Fe_2O_3 , MnO , and MgO relative to UCC (**Figures 5B,C**). The samples from the SD show nearly the same SiO_2 as UCC, but depletion in TiO_2 , Al_2O_3 , Fe_2O_3 , MnO , MgO , Na_2O , and K_2O in contrast to UCC, except for sample SD-6. SD-6 has a high content of MgO . Two samples (SD-1 and SD-5) have lower CaO concentrations compared with UCC, whereas other samples from the SD have relatively higher CaO contents (**Figure 5D**). For all the samples, CaO has a statistically high negative correlation with SiO_2 ($r = -0.95$, $p < 0.05$, $n = 28$) but weak or no correlations with other major elements (**Supplementary Appendix Table S6**), suggesting that the CaO is mainly derived from the carbonate minerals rather than the silicate minerals (e.g., plagioclase and apatite).

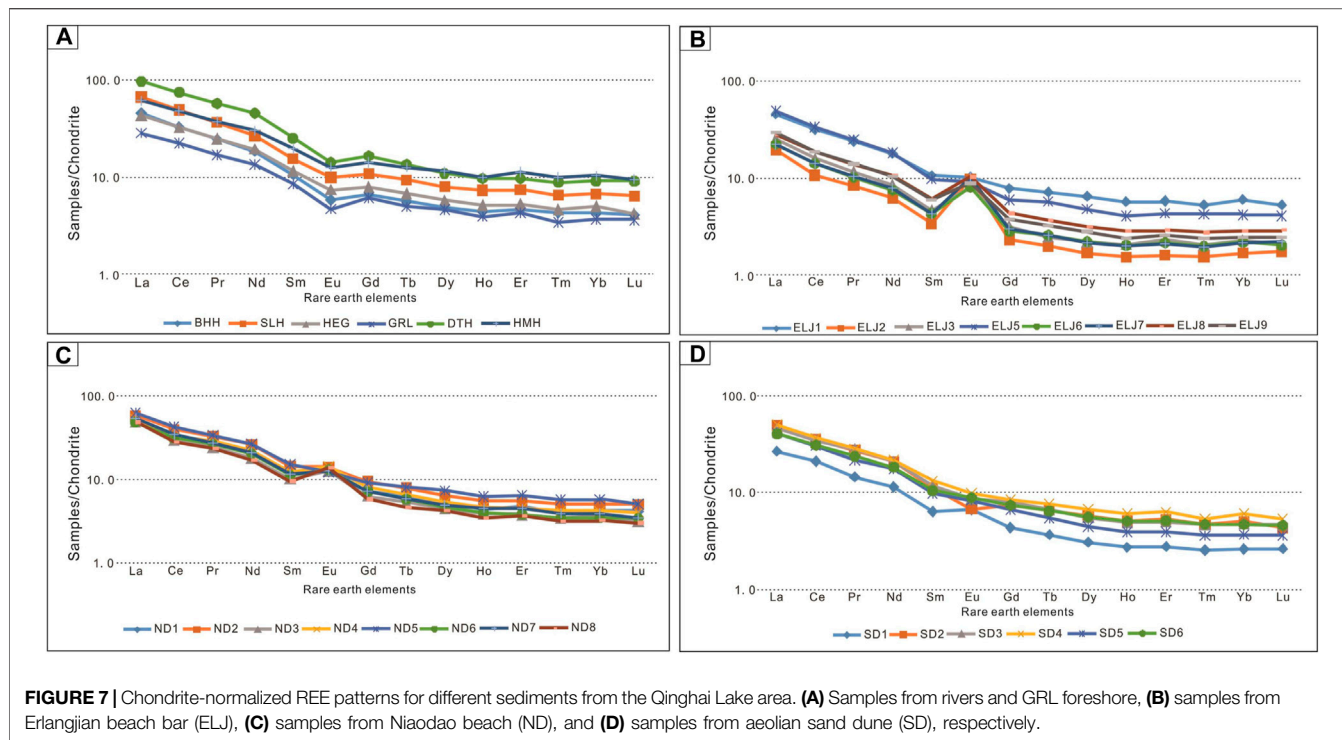
Trace Elements

The selected trace elements of the samples are normalized by UCC and are shown in **Figure 6**. Similar to the UCC-normalized patterns of the major elements, the trace elements from the rivers and GRL vary significantly, whereas the samples from ELJ beach bar, ND beach, and SD show high uniform UCC-normalized patterns. The sample GRL shows a remarkable high Sr concentration relative to UCC, due to its enriched carbonate minerals. Sample DTH has relatively high Zr and Hf concentrations, indicating the sediments are enriched in zircon minerals (**Figure 6A**). The depletion of trace

elements V, Cr, Co, Ni, Cs, Th, U, Nb, Ta, Cu, Zn, Sc, and Ti for most samples is probably due to the grain size of sediments being relatively coarse and lack of fine fractions (Nesbitt et al., 1996). The trace elements Rb, Sr, and Ga are concentrated in the ELJ beach bar, ND beach, and SD samples which is possibly related to the enrichment of K-feldspar minerals (**Figures 6B–D**). The UCC-normalized patterns of the samples of ND beach are a higher degree of uniform than ELJ beach bar and SD, probably indicating that the ND samples are influenced by one major source of rocks, whereas the sand samples from ELJ beach bar and SD are affected by multiple source rocks.

Rare Earth Elements

Compared with UCC (total REE = 148.14 ppm), all the samples have a lower total REE (22.9–142.8 ppm, avg. 63.2 ppm) (**Supplementary Appendix Table S4**). The chondrite-normalized spider diagrams show that all the samples have steep light rare earth elements (LREEs) distribution patterns and relatively flat heavy rare earth elements (HREEs) styles (**Figure 7**). The $(\text{La}/\text{Yb})_N$ values for different samples are 5.9–10.6 with an average of 8.7 for the rivers and GRL, 7.6–12.0 with an average of 10.5 for the ELJ beach bar, 10.6–15.1 with an average of 12.9 for the ND beach, and 8.2–11.1 with an average of 9.6 for the SD, respectively (**Supplementary Appendix Table S4**). Compared with UCC [$(\text{La}/\text{Yb})_N = 10.5$], the samples from ND beach are characterized with a higher degree of REE fractionation, while the samples from the rivers and GRL define relatively less fractionated REE patterns. The samples from the rivers and GRL



are characterized with negative Eu anomalies (0.64–0.77, avg. 0.70) (Figure 7A). Nevertheless, the samples from ELJ beach bar and ND beach show positive Eu anomalies (Figures 7B–D), which is probably due to their high contents of feldspar minerals (Figure 3).

DISCUSSION

Weathering and Sediment Recycling of the Sediments

During the processes of the sediments transferred from the source area to the basin, some elements (e.g., Na, K, and Ca) can be easily dissolved into the water and run away from the sediments, while some other elements (e.g., Al and Ti) are chemically stable and can be retained in the residual minerals. The chemical migration abilities of different elements are closely related to the weathering conditions that the sediments experienced before reaching the final deposition sites (Nesbitt et al., 1980; Fedo et al., 1996). The chemical index of alteration (CIA) is a widely used proxy to evaluate weathering intensity of the sediments underwent during the whole process from the source to the basin (Nesbitt and Young, 1982). The CIA is calculated by using the molecular concentrations of the major elements, and the formula is defined as $CIA = [Al_2O_3 / (Al_2O_3 + CaO^* + Na_2O + K_2O)] \times 100$, where CaO^* represents the amount in silicates only. The CaO correction law follows the method proposed by Fedo et al. (1995), in which when $CaO < Na_2O$, the CaO is used in the CIA formula while when $CaO > Na_2O$, the CaO in the CIA formula will be replaced by Na_2O .

The values of CIA are listed in **Supplementary Appendix Table S7**. The CIA of 37 for sample GRL is the lowest among all the samples, whereas the CIA values for the rivers are slightly greater

than 50, except for sample BHH (42) and the samples from ELJ beach bar, ND beach, and SD are all between 40 and 50 with a mean value of 46. Fedo et al. (1995) suggested that $CIA = 50–60$ is low-intensity weathering, $CIA = 60–80$ is intermediate intensity weathering, and $CIA > 80$ is high-intensity weathering. Therefore, the CIA values of the samples reflect that the sediments experienced low-intensity chemical weathering. The CIA values of the fine-grained Qinghai Lake bottom sediments are 50–59 with an average of 54 (Jin et al., 2009) and the CIA values of loess samples from the eastern margin of the lake are 53–66 with an average of 61 (Zeng et al., 2015) also supporting that the sediments in the Qinghai Lake underwent a low-intensity weathering. The climate conditions in the source area around Qinghai Lake are cold and arid (Xu et al., 2010), which is not beneficial for the strong chemical weathering (McLennan et al., 1993). The chemical weathering unstable minerals (e.g., carbonate, plagioclase, pyroxene, and hornblende) are commonly visible from the thin-sections observation and XRD results also reflect that the sediments of Qinghai Lake experienced low-intensity chemical weathering.

Some heavy minerals (e.g., zircons) can be accumulated during the processes of sediments recycling, which may cause the Zr and Th elements to increase (McLennan et al., 1993). Since Th is typically an incompatible element and Sc is typically compatible in igneous rocks, Th/Sc ratio is an overall indicator of igneous chemical differentiation processes (Taylor and McLennan, 1985). Moreover, zircon addition resulting from sediment recycling and sorting can lead to Th/Sc and Zr/Sc ratios not following the normal igneous differentiation trend (McLennan et al., 1993). Therefore, the diagram of Zr/Sc versus Th/Sc is widely used to assess sediments recycling (McLennan, 1989). On the plot of Zr/Sc versus Th/Sc (Figure 8A), the sample GRL locates at the trend

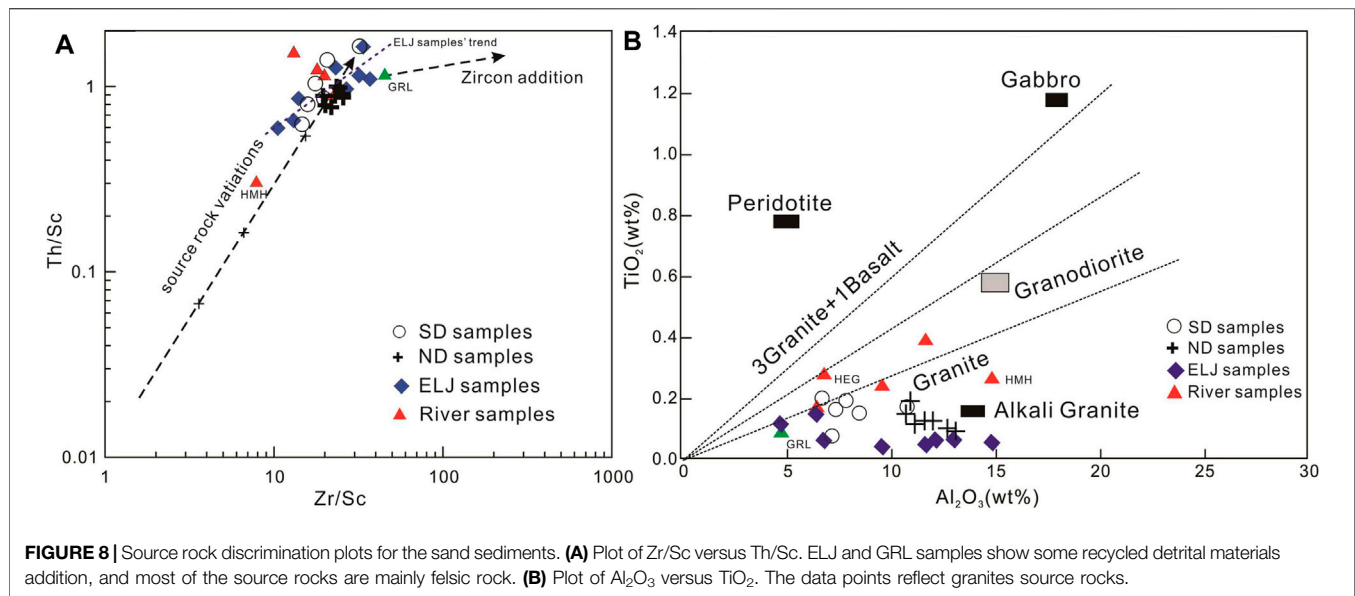


FIGURE 8 | Source rock discrimination plots for the sand sediments. **(A)** Plot of Zr/Sc versus Th/Sc. ELJ and GRL samples show some recycled detrital materials addition, and most of the source rocks are mainly felsic rock. **(B)** Plot of Al_2O_3 versus TiO_2 . The data points reflect granites source rocks.

line of zircon addition, and the samples of ELJ beach bar show a trend of bias to zircon addition, whereas the samples of ND beach and SD are all clustered along with the source rock variation trend line and the river samples (BHH, SLH, HEG, DTH, and HMH) far away from the zircon addition trend line. It means that the sediments from ND beach, SD, and other river samples are not affected by the sedimentary recycling but are only controlled by source rock composition variations. Nevertheless, some recycling materials with zircon addition may be added to the sediments of the ELJ beach bar and GRL area.

Main Source Rocks for the Sediments

Petrographic results show the lithic fragments contained in the sediments mostly carbonate, granite, acid volcanics, siliciclastic rocks, and a few metamorphic rocks (marble and meta-volcanics). Moreover, the XRD results reveal that a certain concentration of calcite, dolomite, pyroxene, and hornblende exist in the sediments besides abundant quartz and feldspar. The above petrology and mineralogy evidence indicates that the source rocks for the Qinghai Lake sediments include at least carbonates, granites, acid volcanic rocks, recycled clastic rocks, and some metamorphic rocks.

Because major elements Al and Ti are immobile and have the lowest solubility in natural water, the ratio of $\text{Al}_2\text{O}_3/\text{TiO}_2$ is widely used to evaluate the source rock types of the sediments. According to Paikaray et al. (2008), the ratio of $\text{Al}_2\text{O}_3/\text{TiO}_2$ below 10 is considered as mafic source rocks, whereas the ratios between 10 and 20 are indicators of intermediate source rocks, and ratios higher than 20 indicate the sediments originated mostly from felsic source rocks. The ratios of $\text{Al}_2\text{O}_3/\text{TiO}_2$ for all the samples are greater than 20 (23.7–249.9, avg. 98.8) indicating that felsic rocks are the primary source rock types. On the plot of Al_2O_3 versus TiO_2 (Figure 8B), most of the samples distributed in the right area of the granite trend line and two samples (HEG and DTH) locate at the area bias to granodiorite line, suggesting that the source rocks are mainly felsic but affected by some intermediate rocks or enriched in titanium minerals.

The ratios of $\text{Al}_2\text{O}_3/\text{TiO}_2$ of the samples from different sites vary greatly. The samples from the rivers and GRL have the lowest $\text{Al}_2\text{O}_3/\text{TiO}_2$ values (23.7–54.9, avg. 38.9) among all the samples, whereas the samples from the ELJ beach bar have the highest $\text{Al}_2\text{O}_3/\text{TiO}_2$ ratios (86.8–249.9, avg. 183.8), and the $\text{Al}_2\text{O}_3/\text{TiO}_2$ values of the samples from ND beach and SD are between the former two sample sites (Supplementary Appendix Table S7). The differences among these sample sites are controlled by the variation of source rock lithic fragments. The thin sections show that the sediments from the rivers and GRL contain the highest contents of source rock lithic fragments, whereas the lithic fragments are few in the samples from the ELJ beach bar (Figure 3B). Furthermore, fine-grained minerals are rarely present in the sediments because of the strong hydraulic conditions. The mafic minerals are preferentially accumulated in fine sands and muds resulting in higher abundances of TiO_2 and FeO in the fine-grained sediments but sand sediments depletion of TiO_2 and FeO (Nesbitt et al., 1996). Therefore, the $\text{Al}_2\text{O}_3/\text{TiO}_2$ ratios of sand would reflect more felsic source rock types. In contrast, the values of $\text{Al}_2\text{O}_3/\text{TiO}_2$ of mud sediments will result in an overestimation of the mafic contribution from source rocks (Nesbitt et al., 1996). For a well understanding of the source rock types, the chemical compositions of simultaneous sand and mud sediments should be taken into account together (Nesbitt et al., 1996). The chemical compositions of fine-grained bottom sediments in Qinghai Lake are referred to by Jin et al. (2009). The $\text{Al}_2\text{O}_3/\text{TiO}_2$ of the bottom sediments in Qinghai Lake are 20.2–23.8, with an average of 22.1 (Jin et al., 2009), also indicating that the source rock types are mainly felsic rocks. In addition, the TiO_2 are highly positively correlated with Fe_2O_3 ($r = 0.93, p < 0.05, n = 28$), Nb ($r = 0.88, p < 0.05, n = 28$), Ta ($r = 0.86, p < 0.05, n = 28$), Zr ($r = 0.90, p < 0.05, n = 28$), and Hf ($r = 0.90, p < 0.05, n = 28$), suggesting that the ilmenite is probably one of the forming minerals for the felsic source rocks.

The trace elements of La, Th, Zr, Hf, Sc, Cr, and Co are geochemically conservative during the surficial processes. La, Th, Zr, and Hf are enriched in felsic rocks. The Sc, Cr, and Co are enriched in mafic rocks. Thus, the ratios of La/Sc, Co/Th, Zr/Sc, and Th/Sc are

widely applied to discriminate the source rock types of clastic sediments. For most of the samples, the ratios of Zr/Sc (avg. 21.38), Th/Sc (avg. 1.01), and La/Sc (avg. 3.72) are higher than those of UCC (13.79, 0.75, and 2.21, respectively) while the Co/Th (avg. 0.88) is lower than UCC (1.65), except for samples GRL, HMH, ELJ-1, and ELJ-7, indicating that the samples' source rocks are more felsic than UCC. The Zr/Sc ratio of sample GRL (Zr/Sc = 13.18) is slightly lower than UCC probably due to the dilution of high contents of carbonate minerals. The sample HMH has the highest Sc, Cr, and Co concentrations among all the samples (**Supplementary Appendix Table S4**), resulting in lower ratios of Zr/Sc (7.93), Th/Sc (0.31), and La/Sc (1.05) and a higher ratio of Co/Th (1.86) than those of UCC, which suggests that the source rocks of the HMH sediments are more mafic than UCC. The thin section shows that the HMH sediments contain abundant mafic minerals (pyroxene and hornblende) (**Figure 2D**), which should be the primary reason for the enrichment in Sc, Cr, and Co. The ratios of Zr/Sc, Th/Sc, La/Sc, and Co/Th of the two samples ELJ-1 and ELJ-7 also reflect the influences of mafic minerals (hornblende), which can be seen in the thin section (**Figures 3C,D**). The mafic materials in the samples ELJ-1 and ELJ-7 should be brought in by the Hema River, which is the mafic materials input water system and the nearest river to the ELJ beach bar (**Figure 1B**).

Implications for the Provenance

The main source rock types for the Qinghai Lake sediments are considered to be felsic rocks according to the bulk geochemical compositions. Integrating with the petrology and mineralogy evidence, a few specific details of the source rocks could be figured out. For example, the marble is one of the source rocks for the sediments from the Haergai River (HEG) according to the thin-section observation; thus, the relatively high CaO content (8.83 wt%) is caused by the marble minerals rather than carbonates. However, the high CaO content (8.65 wt%) in the Buha River (BHH) can explain the existence of carbonate in the source area according to the thin-section observation and petrology analysis. A large amount of biotite and a few hornblende and pyroxene minerals can be observed in the sediments of ELJ beach bar and ND beach, probably indicating that the felsic source rocks are biotite granite or granodiorite with a few basic rocks.

The provenance inferred from the geochemical indicators ($\text{Al}_2\text{O}_3/\text{TiO}_2$, La/Sc, Co/Th, Zr/Sc, and Th/Sc) and petrographic and mineral evidence of the sediments are felsic rocks (granite, granodiorite, and felsic volcanic), carbonate, marble, and a few kinds of basic rocks, which are consistent with the rock types distributed in the mountains around Qinghai Lake (QBGMR, 1991). Nevertheless, the grain sizes of the samples of this study are all relatively coarse representing high hydraulic sorting, which may have an important influence on the geochemical and mineral compositions of the sediments. Previous research suggested that the mafic elements are preferentially enriched in fine-grained sediments (Nesbitt et al., 1996).

CONCLUSION

In this study, the petrology, mineralogy, and bulk geochemical compositions of sand sediments from the five main rivers and

shore-land (beach bar, beach, and aeolian sand dune) of the Qinghai Lake are analyzed. The provenance of the sediments from Qinghai Lake is as follows: 1) the sediments from Qinghai Lake have undergone low-intensity weathering of mostly one single recycling and 2) the source rock types are mainly felsic rocks (granite, granodiorite, and felsic volcanics), carbonate, metamorphic rocks (marble and meta-volcanic rocks), and siliciclastic rocks.

From this work, it can be noted that the indicators of bulk geochemical compositions are useful tools to investigate the source rocks. The petrology of sands can provide some specific and direct evidence for the source rocks. However, the source rock types may be deviated caused by hydraulic sorting if according to only one of the above methods. Thus, the provenance study of the sediments should integrate multiple methods and sediments of all grain sizes (sand, silt, and mud) should be analyzed as far as possible.

DATA AVAILABILITY STATEMENT

The original contributions presented in the study are included in the article/**Supplementary Material**; further inquiries can be directed to the corresponding authors.

AUTHOR CONTRIBUTIONS

HT designed the experiments and wrote this manuscript; LH designed the experiments and collected the samples; SL helped in collecting the samples; TW helped in analyzing the petrography of the samples; ZQ handled the experiments of major and trace elements; and JQ helped in finishing the experiment of trace elements.

FUNDING

The study was supported by the National Natural Funding Science Foundation of China (Grant No: 41502142, 41772142), Key Laboratory Project of Gansu Province (No: 1309RTSA041), Gansu Provincial Natural Sciences (No: 18JR3RA396), and Youth Innovation Promotion Association CAS (No: 2016068).

ACKNOWLEDGMENTS

We would like to thank Professor Yongli Wang and the reviewers for their valuable comments.

SUPPLEMENTARY MATERIAL

The Supplementary Material for this article can be found online at: <https://www.frontiersin.org/articles/10.3389/feart.2021.725553/full#supplementary-material>

REFERENCES

- An, Z. S. (2003). *Scientific Drilling at Qinghai Lake on the Northwestern Tibetan Plateau: High-Resolution Paleoenvironmental Records of Eastern Asia and Their Significance for Global Change Lake Qinghai Workshop*. Xining, China: Institute of Earth Environment, Chinese Academy of Sciences, 1–2
- An, Z., Wang, P., Shen, J., Zhang, Y., Zhang, P., Wang, S., et al. (2006). Geophysical Survey on the Tectonic and Sediment Distribution of Qinghai Lake basin. *Sci. China Ser. D* 49, 851–861. doi:10.1007/s11430-006-0851-1
- Armstrong-Altrin, J. S., Lee, Y. I., Kasper-Zubillaga, J. J., Carranza-Edwards, A., Garcia, D., Eby, G. N., et al. (2012). Geochemistry of beach Sands along the Western Gulf of Mexico, Mexico: Implication for Provenance. *Geochemistry* 72, 345–362. doi:10.1016/j.chemer.2012.07.003
- Armstrong-Altrin, J. S., Lee, Y. I., Verma, S. P., and Ramasamy, S. (2004). Geochemistry of Sandstones from the Upper Miocene Kudankulam Formation, Southern India: Implications for Provenance, Weathering, and Tectonic Setting. *J. Sediment. Res.* 74 (2), 285–297. doi:10.1306/082803740285
- Chang, H., An, Z., and Wu, F. (2008). Major Element Records from the Qinghai lake basin-Gonghe basin Sediments Indicating the Nanshan (Qinghai) Uplift Event. *Quat. Sci.* 28 (5), 822–830.
- Chen, J. (2016). *The Study on Modern Sedimentary System in the Qinghai Lake*. Beijing, China: Ph.D. Thesis, China University of Geosciences
- Cullers, R. L. (2002). Implications of Elemental Concentrations for Provenance, Redox Conditions, and Metamorphic Studies of Shales and Limestones Near Pueblo, CO, USA. *Chem. Geology*. 191, 305–327. doi:10.1016/s0009-2541(02)00133-x
- Dong, H., Song, Y., and Zhang, M. (2019). Hydrological Trend of Qinghai Lake over the Last 60 years: Driven by Climate Variations or Human Activities? *J. Water Clim. Change* 10 (3), 524–534. doi:10.2166/wcc.2018.033
- Fedo, C. M., Eriksson, K. A., and Krogstad, E. J. (1996). Geochemistry of Shales from the Archean (~3.0 Ga) Buhwa Greenstone Belt, Zimbabwe: Implications for Provenance and Source-Area Weathering. *Geochimica Et Cosmochimica Acta* 60, 1751–1763. doi:10.1016/0016-7037(96)00058-0
- Fedo, C. M., Wayne Nesbitt, H., and Young, G. M. (1995). Unraveling the Effects of Potassium Metasomatism in Sedimentary Rocks and Paleosols, with Implications for Paleoweathering Conditions and Provenance. *Geol* 23, 921–924. doi:10.1130/0091-7613(1995)023<0921:uteopm>2.3.co;2
- Hofmann, A., Bolhar, R., Dirks, P., and Jelsma, H. (2003). The Geochemistry of Archean Shales Derived from a Mafic Volcanic Sequence, Belingwe Greenstone belt, Zimbabwe: Provenance, Source Area Unroofing and Submarine versus Subaerial Weathering. *Geochimica Et Cosmochimica Acta* 67, 421–440. doi:10.1016/s0016-7037(02)01086-4
- Jin, Z., An, Z., Yu, J., Li, F., and Zhang, F. (2015). Lake Qinghai Sediment Geochemistry Linked to Hydroclimate Variability since the Last Glacial. *Quat. Sci. Rev.* 122, 63–73. doi:10.1016/j.quascirev.2015.05.015
- Jin, Z., You, C.-F., and Yu, J. (2009). Toward a Geochemical Mass Balance of Major Elements in Lake Qinghai, NE Tibetan Plateau: A Significant Role of Atmospheric Deposition. *Appl. Geochem.* 24, 1901–1907. doi:10.1016/j.apgeochem.2009.07.003
- Lanzhou Institute of Geology, Chinese Academy of Sciences (1979). *Qinghai Lake Integrated Investigation Report*. Beijing: Science Press, 1–270.
- Lee, Y. I. (2009). Geochemistry of Shales of the Upper Cretaceous Hayang Group, SE Korea: Implications for Provenance and Source Weathering at an Active continental Margin. *Sediment. Geology*. 215, 1–12. doi:10.1016/j.sedgeo.2008.12.004
- Li, X.-H. (1997). Geochemistry of the Longsheng Ophiolite from the Southern Margin of Yangtze Craton, SE China. *Geochem. J.* 31, 323–337. doi:10.2343/geochemj.31.323
- Li, Y. T., Li, X.-Y., and Cui, B. (2010). Trend of Streamflow in Lake Qinghai basin during the Past 50 Years (1956–2007): Take Buha River and Shaliu River for Examples. *J. Lake Sci.* 22, 757–766.
- Liu, X., Shen, J., Wang, S., Yang, X., Tong, G., and Zhang, E. (2002). A 16000-year Pollen Record of Qinghai Lake and its Paleocli-Mate and Paleoenvironment. *Chin. Sci Bull* 47, 1931. doi:10.1360/02tb9421
- McLennan, S. M. (1989). Chapter 7. RARE EARTH ELEMENTS IN SEDIMENTARY ROCKS: INFLUENCE of PROVENANCE and SEDIMENTARY PROCESSES. *Rev. Mineralogy Geochem.* 21, 169–200. doi:10.1515/9781501509032-010
- McLennan, S. M., Hemming, S., McDaniel, D. K., and Hanson, G. N. (1993). *Geochemical Approaches to Sedimentation, Provenance, and Tectonics*. Boulder, CO: Geological Society of America Special Papers, 21–40. doi:10.1130/spe284-p21
- Nesbitt, H. W., Markovics, G., and price, R. C. (1980). Chemical Processes Affecting Alkalis and Alkaline Earths during continental Weathering. *Geochimica Et Cosmochimica Acta* 44, 1659–1666. doi:10.1016/0016-7037(80)90218-5
- Nesbitt, H. W., and Young, G. M. (1982). Early Proterozoic Climates and Plate Motions Inferred from Major Element Chemistry of Lutites. *Nature* 299, 715–717. doi:10.1038/299715a0
- Nesbitt, H. W., Young, G. M., McLennan, S. M., and Keays, R. R. (1996). Effects of Chemical Weathering and Sorting on the Petrogenesis of Siliciclastic Sediments, with Implications for Provenance Studies. *J. Geology*. 104, 525–542. doi:10.1086/629850
- Paikaray, S., Banerjee, S., and Mukherji, S. (2008). Geochemistry of Shales from the Paleoproterozoic to Neoproterozoic Vindhyan Supergroup: Implications on Provenance, Tectonics and Paleoweathering. *J. Asian Earth Sci.* 32, 34–48. doi:10.1016/j.jseas.2007.10.002
- Pe-Piper, G., Triantafyllidis, S., and Piper, D. J. W. (2008). Geochemical Identification of Clastic Sediment Provenance from Known Sources of Similar Geology: The Cretaceous Scotian Basin, Canada. *J. Sediment. Res.* 78, 595–607. doi:10.2110/jsr.2008.067
- QBGMR (1991). *Ministry of Geology and Mineral Resources of the People's Republic of China, Regional Geology No. 24, Regional Geology of Qinghai Province*. Beijing: Geological Press, 668pp.
- Qiu, Z., and Zou, C. (2020). Unconventional Petroleum Sedimentology: Connotation and prospect. *Acta Sedimentologica Sinica* 38 (1), 1–29.
- Rahman, M. J. J., Xiao, W., Hossain, M. S., Yeasmin, R., Sayem, A. S. M., Ao, S., et al. (2020). Geochemistry and Detrital Zircon U-Pb Dating of Pliocene-Pleistocene Sandstones of the Chittagong Tripura Fold Belt (Bangladesh): Implications for Provenance. *Gondwana Res.* 78, 278–290. doi:10.1016/j.jgr.2019.07.018
- Rudnick, R. L., and Gao, S. (2003). Composition of the continental Crust. *Treatise Geochem.* 3, 1–64. doi:10.1016/b0-08-043751-6/03016-4
- Schneider, S., Hornung, J., Hinderer, M., and Garzanti, E. (2016). Petrography and Geochemistry of Modern River Sediments in an Equatorial Environment (Rwenzori Mountains and Albertine Rift, Uganda) - Implications for Weathering and Provenance. *Sediment. Geology*. 336, 106–119. doi:10.1016/j.sedgeo.2016.02.006
- Song, Y., Zong, X., Qian, L., Liu, H., and Dong, J., 2020. Minerals Mineralogical Record for Stepwise Hydroclimatic Changes in lake Qinghai Sediments since the Last Glacial Period. *Minerals*, 10(11): 963. doi:10.3390/min10110963
- Taylor, S. R., and McLennan, S. M. (1985). *The continental Crust: Its Composition and Evolution*. Oxford: Blackwell, 312pp.
- Wanas, H. A., and Abdel-Maguid, N. M. (2006). Petrography and Geochemistry of the Cambro-Ordovician Wajid Sandstone, Southwest Saudi Arabia: Implications for Provenance and Tectonic Setting. *J. Asian Earth Sci.* 27 (4), 416–429. doi:10.1016/j.jseas.2005.05.002
- Xiao, J., Jin, Z., Zhang, F., and Wang, J. (2012). Major Ion Geochemistry of Shallow Groundwater in the Qinghai Lake Catchment, NE Qinghai-Tibet Plateau. *Environ. Earth Sci.*, 1331–1344. doi:10.1007/s12665-012-1576-4
- Xu, H., Liu, X. Y., An, Z. S., Hou, Z. H., and Dong, J. B. (2010). Spatial Pattern of Modern Sedimentation Rate of Qinghai Lake and a Preliminary Estimate of the Sediment Flux. *Chin. Sci. Bull.* 55 (7), 621–627. doi:10.1007/s11434-009-0580-x
- Yuan, B., Chen, K., Bowler, J. M., and Ye, S. (1990). The Formation and Evolution of the Qinghai Lake. *Quaternary Sciences. Quat. Sci.* 10, 233–243.
- Zeng, F. M., Liu, X. J., Ye, X. S., and Miao, W. L. (2015). Major Elements of the Eolian Deposits at Zhongyangchang Site in the Qinghai Lake and Their Implication on Chemical Weathering Change. *J. Salt Lake Res.* 23 (1), 1–7.

Zhang, P., Cheng, H., Liu, W., Mo, L., Li, X., Ning, Y., et al. (2019). Geochemical and Isotopic (U, Th) Variations in lake Waters in the Qinghai Lake Basin, Northeast Qinghai-Tibet Plateau, China: Origin and Paleoenvironmental Implications. *Arabian J. Geosciences* 12, 92. doi:10.1007/s12517-019-4255-x

Zhang, P. X., Zhang, B. Z., Qian, G. M., Li, H. J., and Xu, L. M. (1994). The Study of Paleoclimatic Parameter of Qinghai Lake since Holocene. *Quat. Sci.* 3, 225–238.

Conflict of Interest: TW was employed by PetroChina Xinjiang Oilfield Company.

The remaining authors declare that the research was conducted in the absence of any commercial or financial relationships that could be construed as a potential conflict of interest.

Publisher's Note: All claims expressed in this article are solely those of the authors and do not necessarily represent those of their affiliated organizations or those of the publisher, the editors, and the reviewers. Any product that may be evaluated in this article, or claim that may be made by its manufacturer, is not guaranteed or endorsed by the publisher.

Copyright © 2021 Tao, Hao, Li, Wu, Qin and Qiu. This is an open-access article distributed under the terms of the Creative Commons Attribution License (CC BY). The use, distribution or reproduction in other forums is permitted, provided the original author(s) and the copyright owner(s) are credited and that the original publication in this journal is cited, in accordance with accepted academic practice. No use, distribution or reproduction is permitted which does not comply with these terms.